Rice

RESEARCH Open Access

RNA-seq Analysis of the Mechanisms Underlying Chalky Grain and Characterization of Two IAA Receptor Proteins OsAFB3 and OsAFB5 in Chalkiness Formation in *Oryza sativa*

Shaojie Shi[1], Huiying Wang[1], Wenjun Zha[1], An Huang[1,3], Ziyi Chen[1,3], Yan Wu[1], Junxiao Chen[1], Changyan Li[1], Bian Wu[1], Sanhe Li[1], Huashan Xu[1], Peide Li[1], Kai Liu[1], Zhijun Chen[1], Guocai Yang[1*], Lei Zhou[1,2*] and Aiqing You[1,2*]

Abstract

Grain chalkiness is an undesirable agronomic trait that negatively affects both the yield and quality of rice (*Oryza sativa*). The molecular mechanisms underlying chalky grain phenotype have remained largely unclear. In this study, we selected the rice variety HK300 with a high chalkiness, and ZR24D with a low chalkiness, as experimental materials and systematically characterized the reasons of grain chalkiness formation at molecular level by means of RNA-seq analysis. Analysis results revealed that the differentially expressed genes (DEGs) in these two rice varieties were significantly enriched in transcriptional regulation, sucrose and starch metabolism, and phytohormone signal transduction. Moreover, we found the expression of 13 genes related to trehalose pathway (4 out of 14 *TPS* genes and 9 out of 13 *TPP* genes in rice genome) were significantly different between the two varieties, indicating trehalose synthesis pathways may contribute to the increased chalkiness formation. Notably, the number of DEGs associated with the signal transduction pathway for indole-3-acetic acid (IAA), which has been rarely studied for its involvement in chalkiness formation, was the highest among those associated with plant hormone signal transduction. Among them, the expression of two IAA receptor genes, *OsAFB3* and *OsAFB5*, were significantly lower in HK300 than that in ZR24D through RNA-seq and qRT-PCR. Furthermore, we newly validated the two genes negatively regulated the formation of chalkiness through gene knockout. Our findings provided the theoretical basis and novel gene resources for molecular breeding aimed at improving rice quality.

†Shaojie Shi, Huiying Wang, and Wenjun Zha have contributed equally to this work.

*Correspondence:
Guocai Yang
yangguocai1971@163.com
Lei Zhou
zhoulei@hbaas.com
Aiqing You
aq_you@hbaas.com

Full list of author information is available at the end of the article

Keywords Rice, Chalkiness, Grain quality, IAA signal transduction, Breeding

Introduction

Rice is the staple food for over the half of the world population (Yang et al. 2021). Historically, breeders have focused on increasing rice yields to satisfy the escalating food demands of a growing population (Yang et al. 2021). Advances in breeding technology, particularly the use of heterosis, have substantially enhanced these yields (Gong et al. 2017). However, as living standards improve, the demand for high-quality rice is gradually rising. Thus, breeders are now also prioritizing improvements in rice quality (Gao et al. 2024). Quality traits of rice include its appearance, milling properties, nutritional value, and cooking and eating characteristics (Custodio et al. 2019). A key quality issue is chalkiness-an opaque feature in the rice endosperm that negatively affects its appearance and its milling, cooking, and eating quality (Misra et al. 2019). Thus, reducing chalkiness in rice grain is essential for enhancing their overall quality.

The chalkiness formation in rice is closely associated with the development of its endosperm, which undergoes four stages: coenocyte stage, cellularization stage, aleurone layer and starchy endosperm cells differentiation stage, and stored substances accumulation stage (Wu et al. 2016). This process is governed by multiple genes. *OsKRP1*, *OsKRP2*, *OsENL1* and *OsGCD1* are all involved in the regulation of cell cycle, loss function of those genes results in abnormal endosperm development (Hara et al. 2015; Huang et al. 2017; Ajadi et al. 2019). MADS-box family transcription factors (TFs) play a role in cellularization and storage material accumulation regulation. Dysregulation of *OsMADS78*, *OsMADS79* and *OsMADS87* accelerates the cellularization process in rice endosperm, resulting in impaired starch granules (SGs) (Chen et al. 2016; Paul et al. 2020). *OsMADS1*, *OsMADS7* and *OsMADS29*, affect the content of starch and the fine structure of SGs in the endosperm through regulating starch synthesis genes expression (Zhang et al. 2018; Liu et al. 2023a, b).

Starch is the predominant storage substance in rice endosperm, comprising more than 80% of its dry weight (Fan et al. 2022). Several genes, such as *OsGIF2*, *OsAGPS2b* and *OsAGPL2*, encoding ADP-glucose pyrophosphorylase (AGP) subunits, are essential for starch synthesis in rice endosperm (Wei et al. 2017). Loss function of these genes resulted in the obstruction of starch synthesis and chalkiness worsened (Wei et al. 2017). Waxy (*Wx*) genes encode granule-bound starch synthase I (GBSSI), which utilizes ADP-glucose to synthesize amylose in the endosperm. To date, at least nine allelic variations at the *Wx* loci have been identified, with the content of amylose and the structure of SGs closely associated with these variations (Tang et al. 2024). Amylopectin is typically synthesized from adenosine diphosphate glucose (ADPG) through the catalytic actions of soluble starch synthase (SS), starch branching enzyme (SBE), and debranching enzyme (DBE) (Huang et al. 2021). Abnormal expression of genes encoding these enzymes can lead to abnormal SG structure (Chao et al. 2019; Jin et al. 2023).

Trehalose is a stable non-reducing disaccharide that is mainly synthesized in plants through the trehalose-6-phosphate synthase/trehalose-6-phosphate phosphatase (TPS/TPP) pathway (Martins et al. 2013). In *Arabidopsis*, trehalose-6-phosphate (T6P), the core intermediate product in the trehalose synthesis pathway, regulates starch metabolism through posttranslational redox activation of AGPase and starch degradation (Kolbe et al. 2005; Martins et al. 2013). In cereals, TPP/TPS pathway is involved in the regulation of grain phenotypes formation, and apart from the known molecular mechanism of *TaTPP-7 A* in wheat regulating starch synthesis and grain filling mainly through T6P-SnRK1 pathway and sugar-ABA interaction, other regulatory modes are still sketchy (Li et al. 2019; Liu et al. 2023a, b; Miret et al. 2024).

Indole-3-acetic acid (IAA) is an important signaling molecule, essential for development processes in higher plants (Zhang et al. 2020). Quantitative studies on IAA in rice endosperm have shown that the content vary with endosperm development (Kabir et al. 2017). The synthesis of IAA is activated at 3 days after flowering (DAF), and as storage substances accumulate, the IAA content in the endosperm also increases rapidly (Zhang et al. 2020). OsTAR1, OsYUC9 and OsYUC11 are the key enzymes in the IAA biosynthesis. In the mature seeds of *osyuc11* mutant, SGs were loosely packed and many grains appeared chalky (Xu et al. 2021). Similarly, the *ostar1* and *osyuc9* strains exhibited increased grain chalkiness comparable with the *osyuc11* mutant (Xu et al. 2021). The IAA signaling transduction has also been extensively studied, mainly involves three types of proteins: SCFTIR1/AFB E3 ubiquitin ligases (encoded by *TIR1*/*AFB* genes), Aux/IAA repressor proteins and auxin response factors (ARFs). ARF proteins bind to promoters to activate or repress target genes. Aux/IAA repressor proteins inhibit ARF proteins activity. TIR1/AFB proteins, which are receptors for IAA, mediate the ubiquitination and subsequent degradation of Aux/IAA proteins, thus freeing ARF to regulate gene expression (Shi et al. 2023). However, there is limited research on the involvement of IAA signaling transduction pathway in the formation of rice chalkiness.

The findings of extensive research indicate that rice quality formation is a complex process, determined by multiple biological pathways. Here, we examined a rice variety, HK300, exhibits poor quality traits, particularly severe chalkiness, with a chalky grain rate exceeding 98%. To investigate the mechanisms underlying chalkiness in HK300 and to enhance rice quality, we used ZR24D as a control, which has a significantly lower chalky grain rate of 8.4%, and RNA-seq was conducted on seeds from both HK300 and ZR24D at 5, 7 and 10 DAF. Our enrichment analysis revealed significant activity in gene ontology (GO) terms related to transcription regulator activity and DNA-binding transcription factor activity and Kyoto Encyclopedia of Genes and Genomes (KEGG) pathways involved in starch and sucrose metabolism as well as plant hormone signal transduction. Differentially expressed genes (DEGs) analysis indicated significant changes in the expression of genes associated with early endosperm development, carbon partitioning, sugar transport, starch biosynthesis and degradation, storage material accumulation, the trehalose pathway, and phytohormone signal transduction throughout seed development. Moreover, we newly confirmed that two IAA receptor proteins, OsAFB3 and OsAFB5, which are involved in IAA signal transduction, negatively regulated rice chalkiness. Our findings systematically clarified the potential molecular mechanisms underlying chalkiness formation and provide a theoretical basis and new genetic resources for improving rice quality.

Materials and methods

Plant Materials

ZR24D, a rice variety with a low percentage of chalky grains, was obtained from the Rice Research Institute at the Guangxi Academy of Agricultural Sciences in Guangxi, China. By contrast, HK300, a rice variety with a high percentage of chalky grains, was obtained from Guangdong Gudao Agriculture Co., Ltd. Nipponbare served as the genetically modified background material. *osafb3-5* and *osafb3-6* were the homozygous knock out lines of *OsAFB3*, and *osafb5-9* and *osafb5-10* were the homozygous knock out lines of *OsAFB5*. All these materials were cultivated under normal field management conditions at the experimental field of the Grain Crop Research Institute of the Hubei Academy of Agricultural Sciences, Hubei, China.

Phenotypic Evaluation

The grain length, width, and thickness of mature and plump seeds from each strain were measured using a vernier caliper. At least 50 seeds from each line were measured. The 1000-grain weight was determined by weighing 1000 seeds from each line using an electronic balance (Sunny Hengping Instrument, FA2004), and this procedure was performed independently three times. Mature and dried seeds were horizontally sliced into approximately 2-mm sections by using a dissecting knife, and these sections were observed and photographed under a stereomicroscope (Leica, S9D). The percentage of chalky grains for each line was assessed by visually examining the proportion of chalky seeds among 50 randomly selected dehulled seeds. This process was repeated independently three times. At maturation stage, at least eight plants of each line in the middle of each plot were sampled and assessed for plant height, tiller number and spike number per plant.

Starch and Protein Content Measurement

Flour from polished rice was used to determine the contents of total starch, amylose, amylopectin, total protein, albumin, prolamin, glutelin, and globulin. The starch contents were quantified using a plant starch content kit (QYS-234027), the amylose content was determined using an amylose content test kit (QYS-234044), and the amylopectin content was measured using an amylopectin content test kit (QYS-234046). All three reagent kits were purchased from Qiyi Biological Technology Co., Ltd (Shanghai, China). The total protein content was measured using a Kjeldahl nitrogen analyzer. The contents of albumin, prolamin, glutelin, and globulin were determined as previously published methods (Hirano et al. 1991).

Scanning Electron Microscopy Observation

Transverse sections (approximately 2 mm) of mature and dried seeds were attached to a sample holder by using conductive adhesive, uniform sprayed with gold using an ion sputtering coating instrument (Quorum SC7620). The SGs in endosperm were observed and photographed under the scanning electron microscope (ZEISS GeminiSEM 300).

Obtaining Transcriptome Data

The development of rice endosperm is typically divided into four stages: coenocytic nuclear division from 0 to 2 DAF, cellularization from 3 to 5 DAF, aleurone and starchy endosperm cells differentiation from 6 to 9 DAF, and storage substances accumulation from 6 to 20 DAF. Nuclear division and endosperm cell formation occur during the initial two stages, whereas starch and other storage substances predominantly accumulate during the latter two stages (Liu et al. 2022b). So, the seeds of ZR24D and HK300 at 5, 7 and 10 DAF were used for RNA-seq. The samples were prepared using the following steps: the number of days' post-bloom for the seeds was marked using marker pens of different colors. Seeds at 5, 7 and 10 DAF were picked, immediately frozen in liquid nitrogen. Then send the sample to Tianjin Smart

Biotech Technology Co., Ltd. for RNA sequencing data acquisition and analysis. Fast Pure Plant Total RNA Isolation Kit (Vazyme, RC401-01) was used to extract RNA from samples, then qualified RNAs were used for RNA-seq libraries construction according to the NEB normal library construction method (Chen et al. 2018), and the sequencing platform was Illumina. The clean data was obtained by screening raw data using Sickle and SeqPrep software, then the clean reads were aligned to the reference genome (Os-Nipponbare version IRGSP-1.0).

Enrichment and Expression Pattern Analysis of DEGs

For each gene, transcript per kilobase per million mapped reads (TPM) based on the number of uniquely mapped reads was used to calculate the expression level. DESeq2 R package were used for screening DEGs, |log2(fold change)| > 1 and False discovery rate (FDR) < 0.05 as the threshold. Methods for KEGG and GO enrichment analyses were consistent with those used in previous study (Shi et al. 2023). The STEM (Short Time series Expression Miner) software performed clustering analysis on DEGs based on their expression trends, parameter settings referred to previous studies, with a p-value < 0.05 as the threshold for screening significant enrichment patterns (Liu et al. 2022a).

Preparation of Low and High Percentage of Chalky Grains Pools

To verify the correlation between the DEGs screened by RNA-seq and chalkiness formation, we constructed an F_2 population with HK300 and ZR24D as parents. The equal amount of seeds of 10 F_2 plants with high percentage of chalky grains (more than 90%) and 10 F_2 plants with low percentage of chalky grains (less than 10%) at 5, 7 and 10 DAF were selected to extract total RNA to construct the high percentage of chalky grains pools (HP-5, HP-7, HP-10) and low percentage of chalky grains pools (LP-5, LP-7, LP-10).

RNA Isolation and Quantitative Real-time PCR

Samples were ground into powder in liquid nitrogen, and total RNA was extracted from the powdered samples by using the RNAsimple Total RNA kit (Tiangen, DP419). The reverse transcription kit (Takara, RR047Q) was used to synthesize the cDNA. Expression levels of genes were detected using quantitative real-time PCR (qRT-PCR) with the Applied Biosystems SYBR Green master mix for product amplification and the CFX96 Real-Time System (Bio-Rad) for signal collection. Three biological replicates were performed for each sample, with *OsActin1* as the reference gene. The relative expression levels of target genes were calculated using $2^{-\triangle\triangle ct}$ method. Primer sequences are listed in Supplementary Table 10.

Gene Knockout Vectors Construction and Transformation

For the construction of knockout vectors for *OsAFB3* and *OsAFB5*, specific target sites (TCGTCCTTGTTGGCTG TCAGGGG for *OsAFB3* and GTCCAGGTCGTCGTCG GTGACGG for *OsAFB5*) were selected. The target site information was provided to Weimi Biotechnology Co., Ltd. for vector construction and genetic transformation. *pYLCRISPR/Cas9Pubi-H* binary vector was used as the vector backbones (Ma et al. 2015), Nipponbare served as the genetic transformation receptor, and mutations were confirmed through sequencing of the target sites.

Subcellular Localization

The subcellular localization of OsAFB3 and OsAFB5 was investigated using the rice protoplast system. Protoplasts were isolated from 1 to 2 week-old seedlings by using a previously described method (Shi et al. 2021). The open reading frame (ORF) sequences that lacking stop codons of *OsAFB3* and *OsAFB5* were inserted into the binary vector *pCXUN*, which fused with a C-terminal GFP tag, and *UBI* promoter driven their expression (Chen et al. 2009). The resulting plasmid vectors were named *OsAFB3-GFP* and *OsAFB5-GFP*. OsbZIP63-RFP was used as a nuclear marker (Shi et al. 2021). Using the polyethylene glycol method, *OsAFB3-GFP* was alone and *OsAFB5-GFP* with the *OsbZIP63-RFP* were co-transfected into the protoplasts. After transfection, the protoplasts were cultured avoid light at 28 °C for 16–24 h. Subsequently, fluorescence in the protoplasts was observed and photographed using a Nikon C2-ER laser scanning confocal microscope.

Prediction of Interacting Proteins

The prediction of interacting proteins in this study was conducted on a multimodal protein interaction intelligent selection platform based on AlphaFold Multimer (Hefei Kejing Biotechnology Co., Ltd). Firstly, the three-dimensional structures of OsAFB3, OsAFB5 and 31 AUX/IAA proteins were constructed using AlphaFold 3. Then, the binding energy between bait protein and prey protein was calculated using HDOCK. It is generally believed that if the Hdock value is less than − 200, two proteins may interact with each other. Finally, the prediction template modeling score (pTM) and interface prediction template modeling score (ipTM) between the two proteins were calculated using AlphaFold 3. If the pTM + ipTM value is greater than 0.75, it indicates good docking effect and reliable results (Yan et al. 2020).

Data Analysis

The significance of differences in the study variables was determined using one-way analysis of variance with PASW Statistics version 18.0.

Results

Assessment of the Grain Chalkiness of HK300 and ZR24D

HK300 and ZR24D are two conventional rice varieties. The grain dimensions of HK300—length (14.83 mm), width (3.26 mm), and thickness (2.61 mm)—were significantly larger than those of ZR24D—length (10.50 mm), width (2.50 mm), and thickness (2.18 mm) (Fig. 1A–E). In addition, the 1,000-grain weight of HK300 was 50.39 g, which was significantly higher than that of ZR24D at 27.90 g (Fig. 1F).

Chalkiness, an undesirable trait, affected rice grain quality and varied considerably between the two cultivars. The percentage of chalky grains in HK300 was 98.4%, significantly higher than that observed in ZR24D (8.4%) (Fig. 1G, J, M). Previous studies have linked chalkiness to the structure and storage materials of seed endosperm (Wu et al. 2022). Thus, we examined the transverse sections of mature seeds from both varieties by using a stereomicroscope. In the mature endosperm of HK300, large white areas were discovered, but there were few white areas in the transverse sections of the ZR24D mature seeds (Fig. 1H, K). Additionally, SGs in the mature endosperm of both varieties were analyzed using scanning electron microscopy. The SGs in HK300 were spherically and loosely arranged, with large air spaces visible (Fig. 1I). By contrast, the SGs in ZR24D were regular and tightly arranged, with no visible spaces (Fig. 1L). The contents of starch and protein in the mature endosperm of HK300 and ZR24D were also measured. The results indicated no significant difference in total starch content between the two varieties (Fig. 1N). However, HK300 exhibited significantly lower amylose content and higher

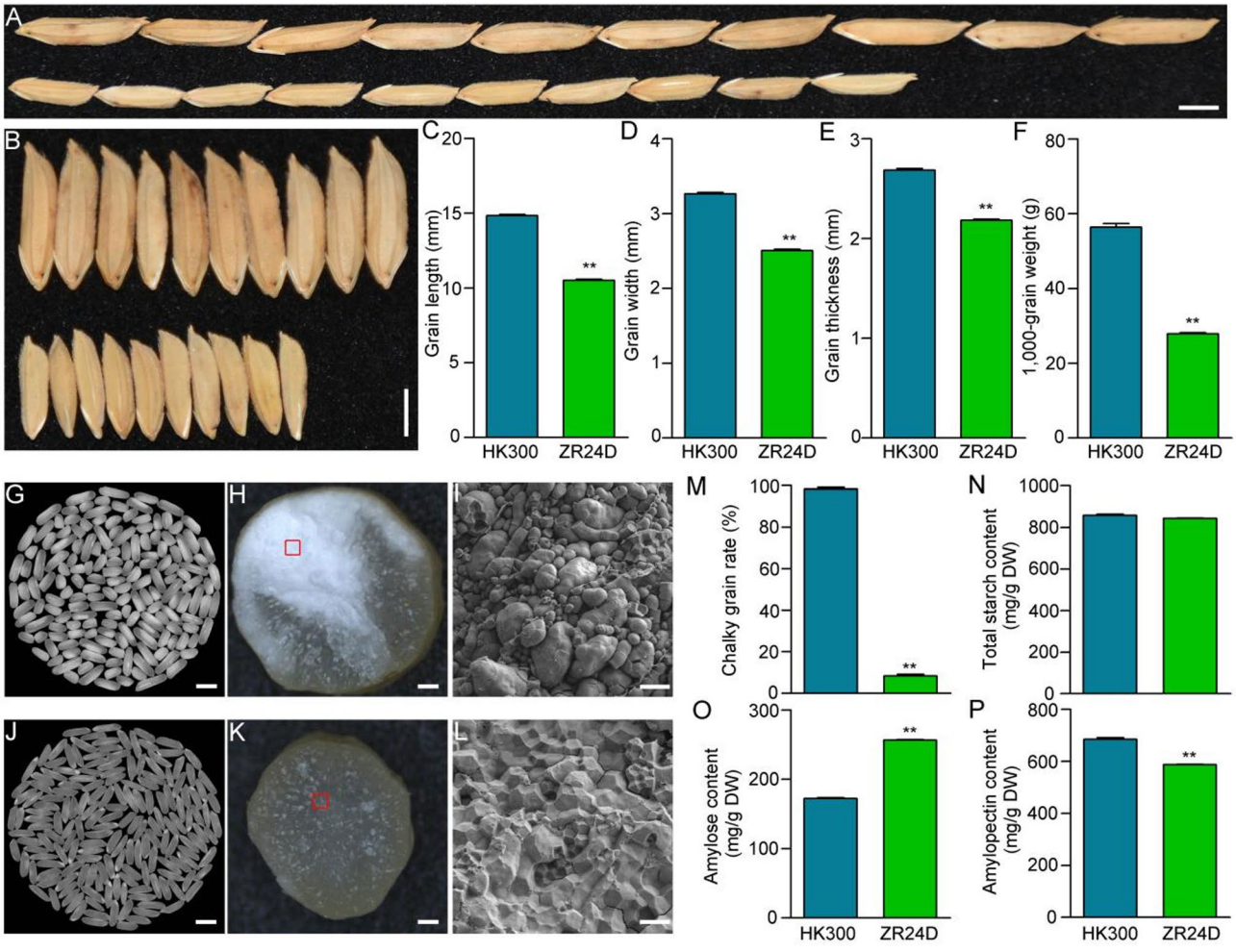

Fig. 1 Phenotypic investigation of HK300 and ZR24D. **A**, **B** Photographs of grain length (**A**) and width (**B**) of HK300 and ZR24D. **C–F** Quantification of grain length (**C**), width (**D**), thickness (**E**) and 1,000-grain weight (**F**) of HK300 and ZR24D. **G** Photograph of HK300 polished rice. **H** Image of transverse sections of HK300 mature seeds obtained by stereomicroscope. **I** Diagram of SGs structure of HK300 marked with the red box in (**H**) obtained by scanning electron microscopy. **J** Photograph of ZR24D polished rice. **K** Image of transverse sections of ZR24D mature seeds obtained by stereomicroscope. **L** Diagram of SGs structure of ZR24D marked with the red box in (**K**) obtained by scanning electron microscopy. **M–P** Quantification of chalky grain rates (**M**), starch contents (**N**), amylose contents (**O**) and amylopectin contents (**P**) of HK300 and ZR24D. In **A**, **B**, **G** and **J**, scale bars, 5 mm; **H**, **K** scale bars, 200 μm; **I**, **L** scale bars, 10 μm. In **C–F**, **M–P**, data represent the means ± SEM. Asterisks indicate significant differences (**$p < 0.01$)

amylopectin content than ZR24D (Fig. 1O, P). Additionally, the total protein content in HK300 was significantly higher than that in ZR24D, while the contents of albumin, prolamin, and globulin were significantly lower, and the glutelin content was substantially higher (Fig. S1).

These findings demonstrate that grain size of HK300 is relatively large and has great potential for increasing yield, but the rice quality, particularly in terms of chalkiness, is more severely compromised in HK300.

Transcriptome Analysis of the Causes of Chalkiness Formation

To investigate the mechanisms behind chalkiness formation in HK300 endosperm, RNA-seq analysis was performed on seeds at 5, 7 and 10 DAF from HK300 (H5, H7, H10) and ZR24D (Z5, Z7, Z10). After removing uncertain reads, low-quality reads, and adapters, a total of 22,029,526–40,199,362 clean reads were obtained, with an average Q30 score ranging from 93.44 to 95.43%. These clean reads were then aligned to the reference genome, achieving alignment rates between 94.27 and 97.75%, and 27,438 genes were identified (Tables S1 and S2). Correlation analysis confirmed strong correlations among three replicates within the same group, indicating strong repeatability among biological replicates and the RNA-seq data was highly accurate (Fig. S2).

To characterize changes in gene expression during endosperm development, we identified DEGs based on the filter criteria of $|\log2(\text{fold change})| > 1$ and FDR < 0.05. In the comparison between H5 and H7, 7863 DEGs were identified, with 3214 DEGs being upregulated and 4649 being downregulated. In the comparison between Z5 and Z7, we identified 5732 DEGs, of which 2115 were upregulated and 3617 were downregulated. In the comparison between H5 and H10, 8300 DEGs were identified, of which 4140 were upregulated and 4160 were downregulated. In the comparison between Z5 and Z10, a total of 6750 DEGs were detected, consisting of 2939 upregulated and 3811 downregulated genes. In the comparison between H7 and H10, 5409 DEGs were identified, of which 3747 were upregulated and 1662 were downregulated. In the comparison between Z7 and Z10, 3063 DEGs were identified, of which 1939 were upregulated and 1124 were downregulated (Fig. 2A, Table S3).

Venn diagrams were performed to illustrate the numbers of overlap and unique DEGs in the two varieties. The results showed that in 5 DAF vs. 7 DAF, 5 DAF vs. 10 DAF and 7 DAF vs. 10 DAF comparison groups, the numbers of DEGs were huge different between the both materials (Fig. 2B). In addition, cluster analysis were conducted based on the expression patterns of all DEGs identified in the two varieties. Then we observed profile 1 was significant enriched in both materials, the highest expression levels of these DEGs at 5 DAF, and then tend to remain unchanged. But profile 2, in which cluster the expression patterns of DEGs were first decline and then increase, was significant enriched in HK300 specifically (Fig. S3). Together, these analyses implied that there were significant differences in the number and expression trends of DEGs during seed development between the two materials.

To elucidate the molecular mechanisms underlying chalkiness formation, GO and KEGG analyses were performed on the identified DEGs. GO enrichment analysis demonstrated that the DNA-binding transcription factor activity and transcription regulator activity within the molecular function category were significantly enriched in all six comparison groups (H5 vs. H7, H5 vs. H10, H7 vs. H10, Z5 vs. Z7, Z5 vs. Z10 and Z7 vs. Z10) (Fig. 2C, Table S4). KEGG analyses revealed significant enrichment in the pathways of starch and sucrose metabolism and plant hormone signal transduction across all the comparison groups (Fig. 2D, Table S5). These enrichment results suggested that genes related to transcription regulation, starch and sucrose metabolism, and plant hormone signal transduction may play crucial roles in endosperm development.

Functional Analysis of TFs during Endosperm Development

Numerous studies have reported the involvement of TFs in the formation of rice chalkiness (Juan et al. 2021). In the DEG analysis, 991 differentially expressed TFs were identified across the six comparison groups and classified into 48 types based on gene annotation (Os-Nipponbare annotation version 2022-09-01 https://rapdb.dna.affrc.go.jp/download/irgsp1.html), including ARF, bHLH, bZIP, ERF, MADS, MYB, NAC, NF-YA, WRKY and YABBY, etc. (Table S6). Venn diagrams revealed that 847 TFs exhibited differential expression in the H5 vs. H7, H5 vs. H10, and H7 vs. H10 groups, whereas 725 TFs showed expression changes in the Z5 vs. Z7, Z5 vs. Z10, and Z7 vs. Z10 comparison groups. A total of 268 and 146 unique differentially expressed TFs were identified during endosperm development of HK300 and ZR24D, respectively. Additionally, 579 differentially expressed TFs were found to overlap in both varieties during endosperm development (Fig. 3A). Based on the expression patterns of differentially expressed TFs in the two varieties, three clustering profiles were significant enriched in HK300, the highest expression levels at 5 DAF and the expression profile 4 tended to decrease in expression during development, the TFs in profiles 1 and 5 showed first decrease and then increase in expression. Nevertheless, there were two significant clustering patterns in ZR24D, the highest expression levels of these TFs at 5 DAF as well, while the expression continues to decline (Fig. 3B). This indicated significant differences were existence in the expression

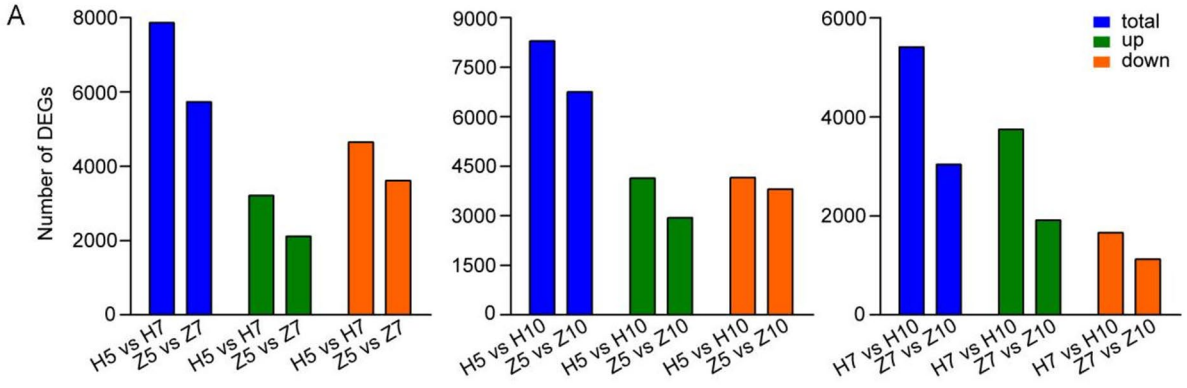

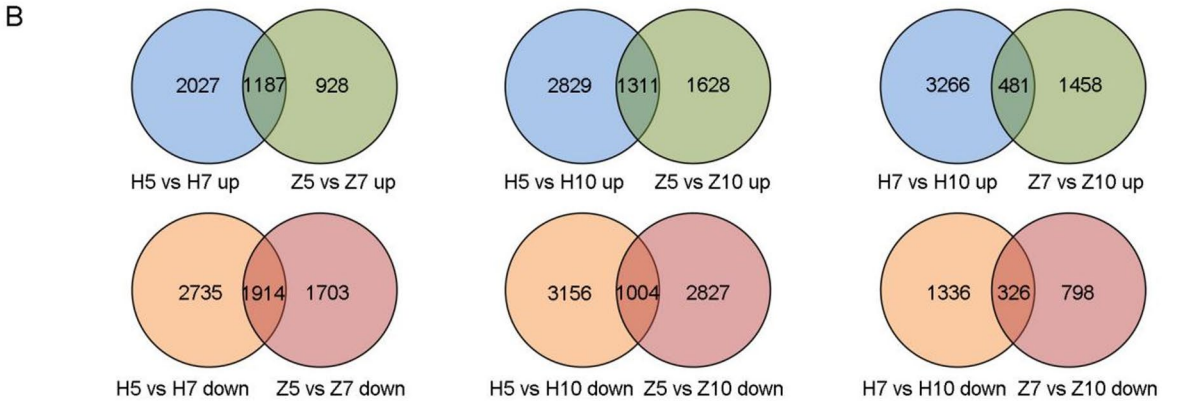

C

GO accession	Go terms	H5 vs H7[a)]	H5 vs H10	H7 vs H10	Z5 vs Z7	Z5 vs Z10	Z7 vs Z10
GO:0003700	DNA-binding transcription factor activity	178	172	141	132	167	73
GO:0140110	transcription regulator activity	183	173	145	134	168	74

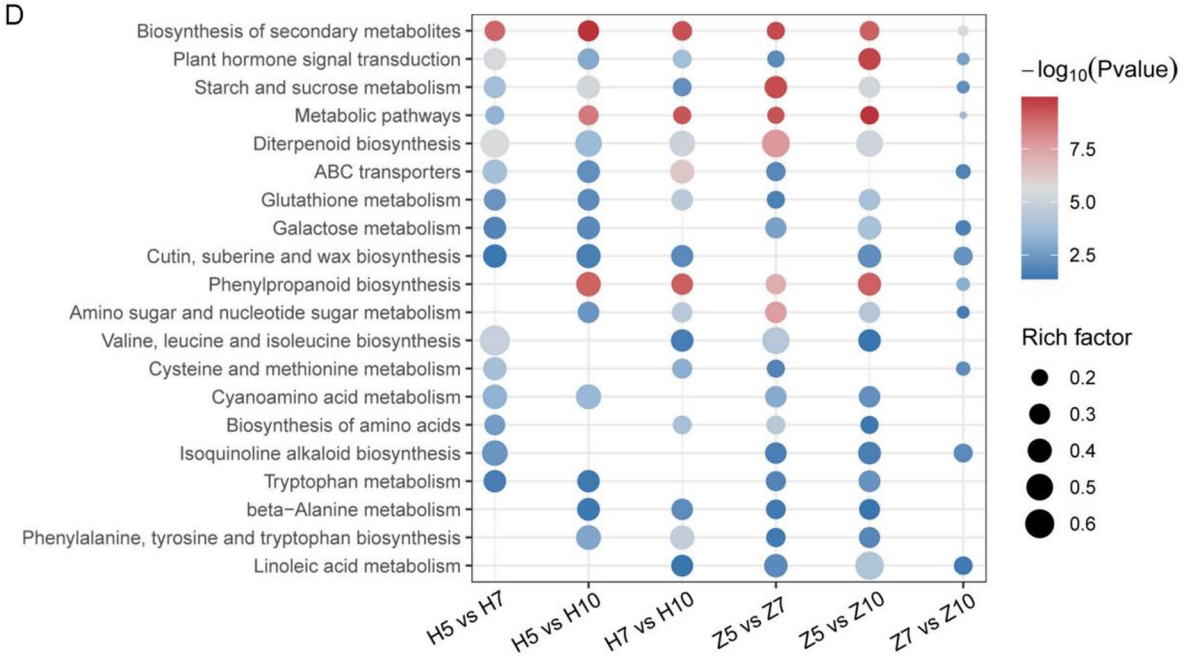

Fig. 2 Differential expression genes (DEGs) analysis. **A** The numbers of total, up- and down-regulated DEGs in the six comparison groups. **B** Venn diagrams illustrated the numbers of overlap and unique DEGs in six comparison groups. **C** Gene ontology (GO) terms DNA-binding transcription factor activity and transcription regulator activity were significantly enriched in all six comparison groups. [a)] indicated the numbers of DEGs related to the corresponding GO terms. **D** Kyoto Encyclopedia of Genes and Genomes (KEGG) enrichment analysis of DEGs from the six comparison groups

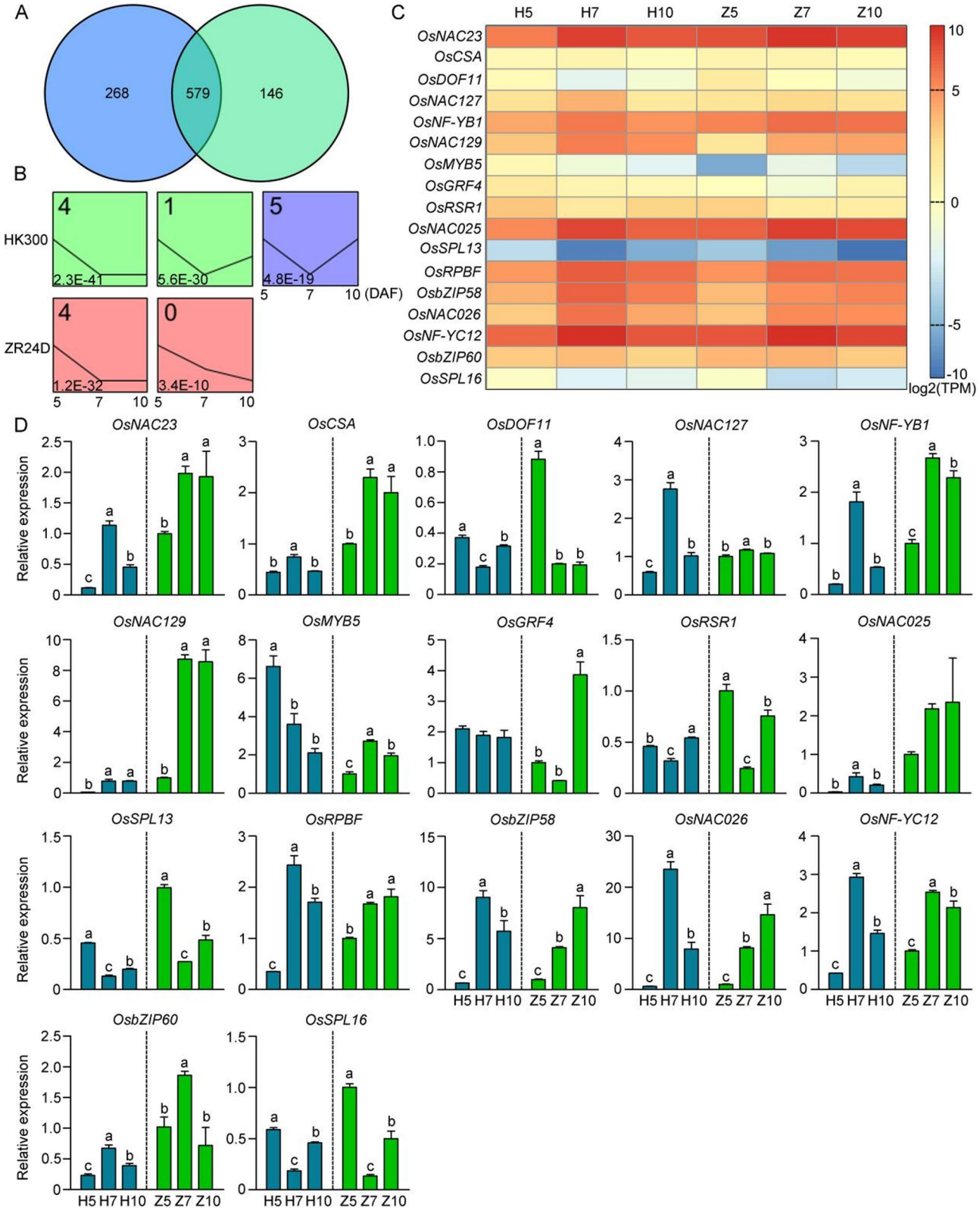

Fig. 3 (See legend on next page.)

(See figure on previous page.)

Fig. 3 Differential expression transcription factors (TFs) analysis. **A** Venn diagrams illustrated the numbers of overlap and unique differential expression TFs in H5 vs. H7, H5 vs. H10, H7 vs. H10 (left) and in Z5 vs. Z7, Z5 vs. Z10, Z7 vs. Z10 (right). **B** The significantly enriched expression pattern clusters of differential expression TFs in HK300 and ZR24D. X axis corresponds to the stages of grain, Y axis represents the expression change of differentially expressed TFs in the two varieties. The fold lines represent the TFs expression trends. The number in the upper left corner represents the expression pattern serial number, and the number in the lower left corner represents the *p*-value of the clustering pattern. **C** Heat map analysis of expression levels of partial TFs in HK300 and ZR24D. **D** qRT-PCR verification of the expression of TFs in HK300 (left, H5/H7/H10) and ZR24D (right, Z5/Z7/Z10). *OsActin1* as the reference gene. Data represent the means ± SEM. Different letters represent significant differences ($p < 0.05$)

levels and trends of TFs during seed development between the two materials.

MADS-box containing TFs, believed to be involved in early endosperm development and regulation of starch metabolism related genes expression, showed varied expression patterns (Juan et al. 2021). Specifically, 31 MADS-box TFs displayed differential expression levels; *OsMADS32* and *OsMADS57* were upregulated in ZR24D but downregulated in HK300. *OsMADS4* and *OsMADS55* showed decreased expression specifically in HK300, whereas the expression of *OsMADS18*, *OsMADS37*, *OsMADS58* and *OsMADS30* exhibited specifically downregulated in ZR24D. In ZR24D, the expression of *OsMADS61* increased, whereas that of *OsMADS73* remained unchanged in ZR24D but increased in HK300 (Fig. S4A). Significant differences in transcript accumulation were also noted in other TFs that have been reported to involve in chalkiness formation during endosperm development of the two varieties (Fu et al. 2010; Wang et al. 2015; Ren et al. 2021; Li et al. 2022) (Fig. 3C). The differential expression of the above genes was verified in the seeds of HK300 and ZR24D through qRT-PCR (Fig. 3D and S4B). To eliminate the interference of genetic backgrounds of the 2 varieties, we also detected the expression level changes of the aforementioned genes in the high and low percentage of chalky grains pools, results showed similar expression trends with the RNA-seq analysis (Table S7). These results together indicated that abnormal regulation of genes expression at any stages of grain development may contribute to the appearance of chalkiness in HK300.

Expression of Many Genes Related To Glycometabolism Were Changed in Chalkiness Formation in HK300

Starch, which constitutes to more than 80% of the dry weight of rice endosperm, is closely linked to grain chalkiness (Fan et al. 2022). In rice endosperm, sucrose is cleaved into glucose and fructose (Fan et al. 2019). These sugars are then converted into starch through the catalytic action of a series of enzymes (Meng et al. 2020; Huang et al. 2021; Liu et al. 2022b). In our DEGs analysis, significant differences in the expression of a large amount of genes involved in sucrose and starch metabolism were discovered during endosperm development in both varieties (Figs. 4A and S5).

Trehalose, a nonreducing glucose disaccharide, affects starch synthesis through the trehalose pathway (Martins et al. 2013). This pathway involves two enzymes: trehalose-6-phosphate synthase (TPS), which catalyzes the movement of glucose from UDPG to glucose-6-phosphate (G6P) to form trehalose-6-phosphate (T6P), and trehalose-6-phosphate phosphatase (TPP), which dephosphorylates T6P to form trehalose (Martins et al. 2013). Our DEGs analysis identified multiple *TPS* and *TPP* genes that were differentially expressed during endosperm development. *OsTPS2* and *OsTPS5* were upregulated in HK300, whereas their expression in ZR24D remained unchanged. *OsTPS7* and *OsTPS8* were downregulated in ZR24D; however, their expression remained unchanged in HK300 (Fig. 4A). The expression patterns of *OsTPP3*, *OsTPP4* and *OsTPP7* were similar in both varieties (Fig. 4A). *OsTPP1*, *OsTPP6* and *OsTPP9* were downregulated in ZR24D, whereas in HK300, *OsTPP1* and *OsTPP6* expressions remained stable but *OsTPP9* was upregulated (Fig. 4A). The expression levels of *OsTPP2*, *OsTPP5* and *OsTPP8* remained unchanged in ZR24D during endosperm development; however, *OsTPP5* and *OsTPP8* were downregulated and *OsTPP2* was upregulated in HK300 (Fig. 4A).

To validate these findings, we selected 30 genes for qRT-PCR analysis in the seeds of HK300 and ZR24D. The qRT-PCR results were consistent with the changes observed in the expression of the aforementioned DEGs (Fig. 4B and S6). In addition, we also detected these genes expression levels in the high and low percentage of chalky grains pools, results showed that the expression trends of the above genes were consistent with the RNA-seq analysis (Table S7). These results collectively indicated that grain chalkiness in HK300 may be related to sucrose metabolism, amylose synthesis, and starch degradation. It was worth noting that during this process, the expression of trehalose synthesis genes undergo significant changes, which may play a significant role in the formation of chalkiness.

IAA Signal Transduction May Play a Major Role in the Formation of Chalkiness

KEGG analysis revealed that a large amount of DEGs involved in plant hormone signal transduction were significantly enriched (Fig. 2D). These DEGs were primarily associated with six hormonal signaling pathways: Abscisic Acid (ABA), brassinolide (BR), ethylene (ET), IAA, jasmonic acid (JA), and salicylic acid (SA) (Fig. 5, Table S8). Notably, the number of DEGs refer to the IAA

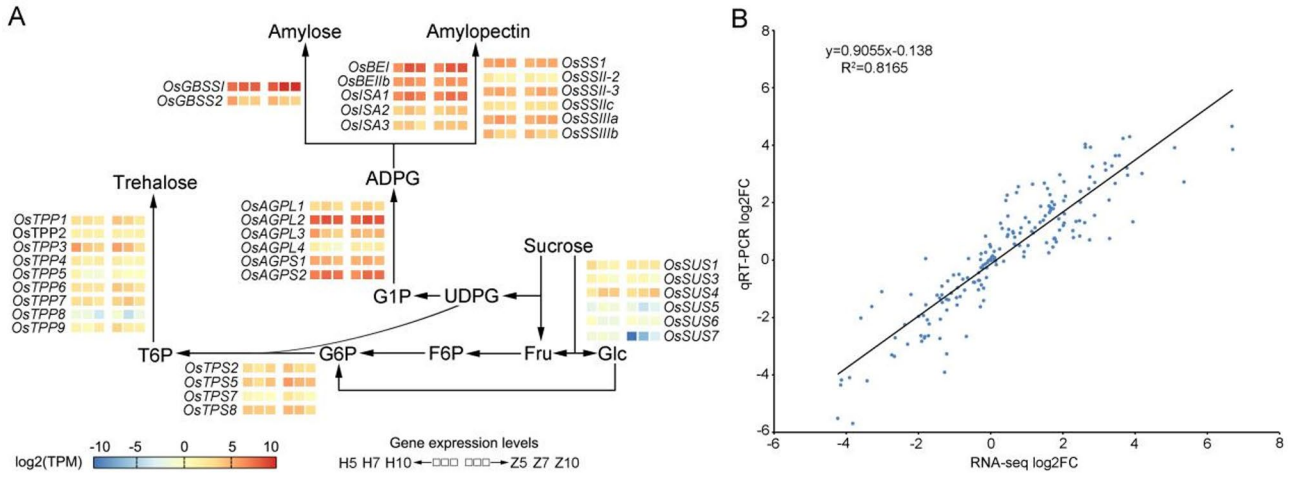

Fig. 4 Expression analysis of starch and sucrose metabolism related genes in HK300 and ZR24D. **A** Reconstruction of the starch and sucrose metabolism pathway with DEGs identified in HK300 and ZR24D. Fru, fructose; Glu, glucose; F6P, fructose-6-phosphate; G6P, glucose-6-phosphate; T6P, trehalose-6-phosphate; UDPG, UDP-glucose; G1P, glucose-1-phosphate; ADPG, adenosine diphosphate glucose. **B** Scatter plot of correlation between gene expression changes measured by RNA-seq and qRT-PCR. *OsActin1* as the reference gene in qRT-PCR. Data represent means of three independent biological repeats. The correlation coefficient is represented by R^2

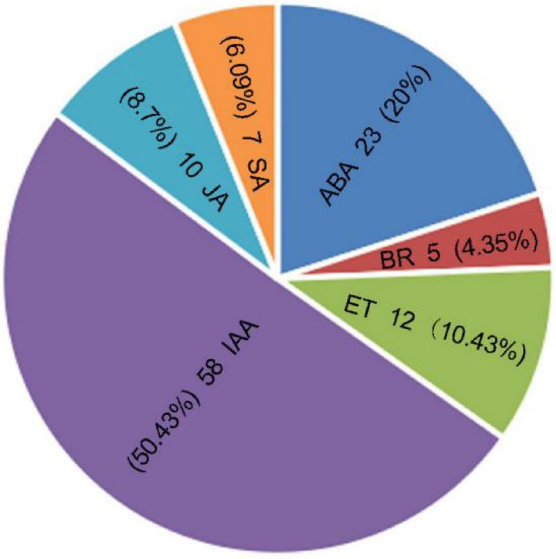

Fig. 5 Number of DEGs related to plant hormone signal transduction pathways in HK300 and ZR24D. The pie chart displays the number of genes involved in ABA, BR, ET, IAA, JA, SA signaling transduction pathways. The number represents the number of DEGs corresponding to hormone signal transduction, percentage represents the proportion of DEGs related to individual hormone signaling pathway to the total DEGs related to hormone signaling pathways

signaling transduction pathway (58/115) was the highest among those associated with plant hormone signal transduction (Fig. 5). In this pathway, multiple genes exhibited varying expression levels during endosperm development in both varieties (Table S8), suggesting that the formation of chalkiness in HK300 may result from the integrated effects of abnormal regulation of hormone signaling, especially the IAA signaling transduction pathway.

IAA Receptor Proteins OsAFB3 and OsAFB5 Negatively Regulated Chalkiness

In our DEGs analysis, the expression levels of *OsAFB3* and *OsAFB5*, which encode IAA receptor proteins, were significantly downregulated in HK300 during endosperm development, whereas no changes were observed in ZR24D (Table S8). Similar trends were qualified by qRT-PCR (Fig. 6A, B). These results indicated *OsAFB3* and *OsAFB5* may be associated with the formation of chalkiness. To investigate the role of *OsAFB3* and *OsAFB5* in the development of grain chalkiness, functional knockout lines under the Nipponbare genetic background were constructed. Among them, two homozygous knockout strains for *OsAFB3* (*osafb3-5* and *osafb3-6*) and for *OsAFB5* (*osafb5-9* and *osafb5-10*) were selected for chalkiness assessment (Fig. 6C). The percentage of chalky grains in *OsAFB3* and *OsAFB5* homozygous knockout lines were exceeded 54.8% and 56% respectively, significantly surpassing the percentage in Nipponbare, in which the rate of chalky grains was only 2.8% (Fig. 6D, E). Transverse sections of mature seeds from the knockout strains revealed large opaque areas, in contrast to the few white areas in Nipponbare (Fig. 6D). Furthermore, SGs in the mature seeds of the knockout strains were irregularly shaped, loosely arranged, and displayed large gaps between SGs, unlike the tightly arranged, regular SGs in Nipponbare (Fig. 6D). These results indicated *OsAFB3* and *OsAFB5* negatively regulated chalkiness in rice.

Starch and protein contents in the mature endosperm of Nipponbare, *osafb3-5*, *osafb3-6*, *osafb5-9* and *osafb5-10* were also measured, which showed no significant differences in the total starch content (Fig. 6F). However, the *OsAFB3* and *OsAFB5* knockout lines exhibited lower

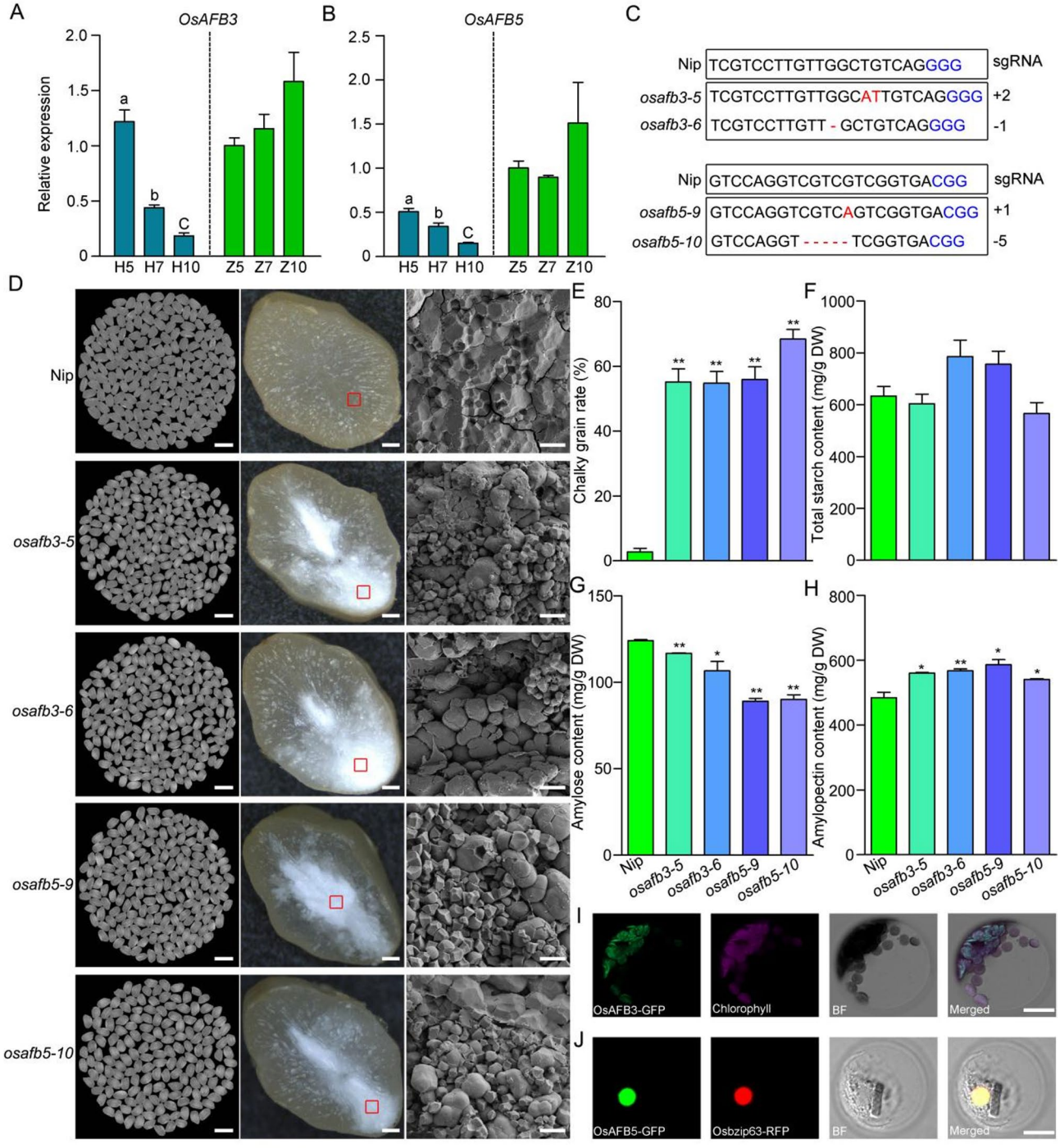

Fig. 6 Functional analysis of *OsAFB3* and *OsAFB5*. **A**, **B** qRT-PCR detection of *OsAFB3* (**A**) and *OsAFB5* (**B**) expression levels in HK300 (left) and ZR24D (right). *OsActin1* as the reference gene. Data represent the means ± SEM. Different letters represent significant differences ($p < 0.05$). **C** The results of DNA sequencing of sgRNA target sites of *OsAFB3* and *OsAFB5*. **D** Photographs of Nipponbare, *OsAFB3* and *OsAFB5* knockout lines polished rice (left), scale bars, 5 mm; Image of transverse sections of Nipponbare, *OsAFB3* and *OsAFB5* knockout lines mature seeds obtained by stereomicroscope (middle), scale bars, 200 μm; Diagrams of SGs structure of Nipponbare, *OsAFB3* and *OsAFB5* knockout lines marked with the red box obtained by scanning electron microscopy (right), scale bars, 10 μm. **E–H** Quantification of chalky grain rates (**E**), starch contents (**F**), amylose contents (**G**) and amylopectin content (**H**) of Nipponbare, *OsAFB3* and *OsAFB5* knockout lines. Data represent the means ± SEM. Asterisks indicate significant differences (*$p < 0.05$, **$p < 0.01$). **I**, **J** Subcellular localization of OsAFB3 (**I**) and OsAFB5 (**J**) in rice protoplasts. BF, Bright-field. Chlorophyll, auto fluorescence signals of chloroplasts. Scale bars, 5 μm

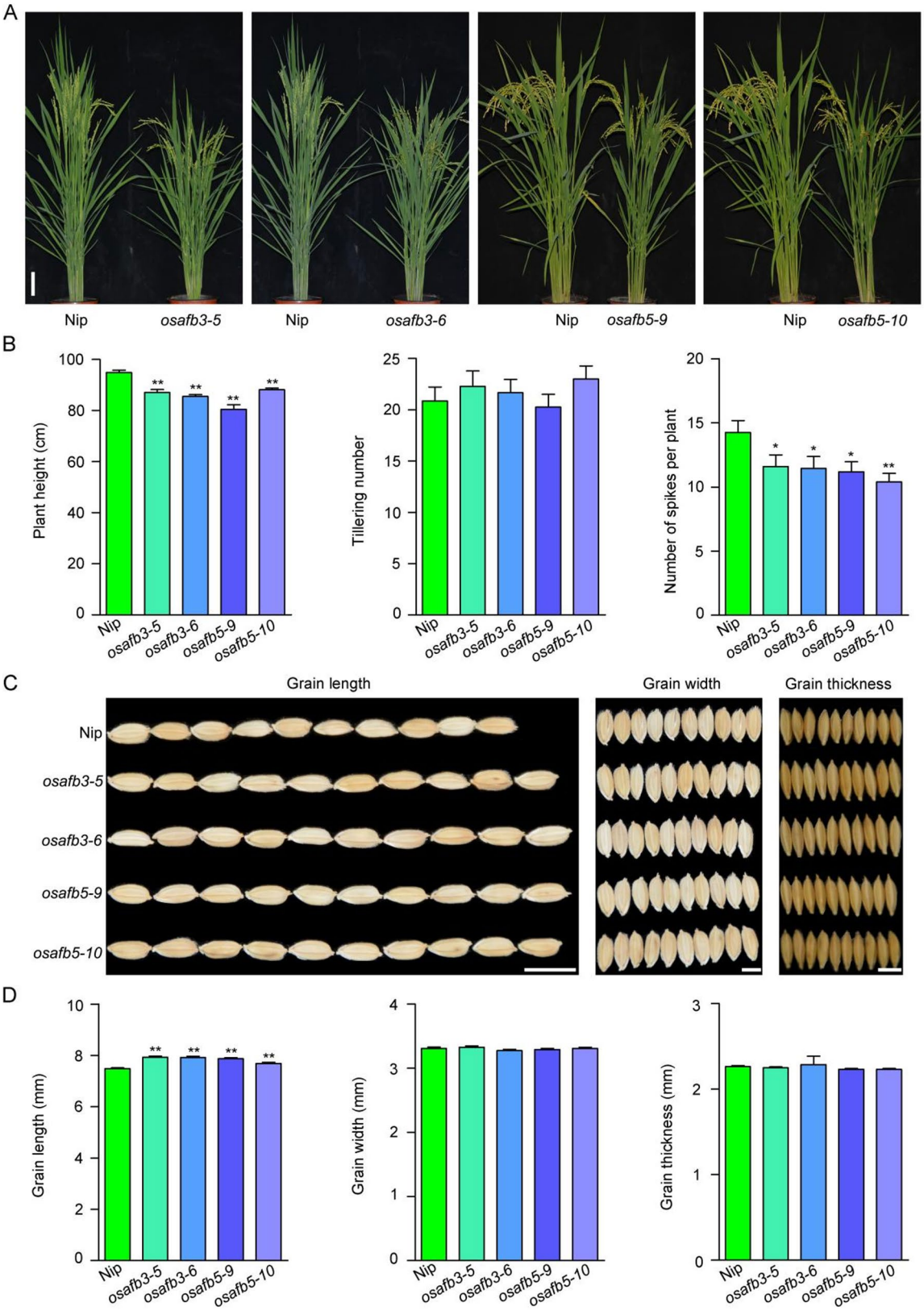

Fig. 7 (See legend on next page.)

(See figure on previous page.)

Fig. 7 Phenotypes of *OsAFB3* and *OsAFB5* knockout lines. **A** Photographs of Nipponbare, *OsAFB3* and *OsAFB5* knockout lines at mature stage. Scale bar, 10 cm. **B** Quantification of plant height, tillering number and panicle number per plant of Nipponbare, *OsAFB3* and *OsAFB5* knockout lines. Data represent the means ± SEM. Asterisks indicate significant differences (*$p < 0.05$,**$p < 0.01$). **C** Photographs of grain length (scale bar, 1 cm), grain width (scale bar, 5 mm) and grain thickness (scale bar, 5 mm) of Nipponbare, *OsAFB3* and *OsAFB5* knockout lines. **D** Quantification of grain length, width and thickness of Nipponbare, *OsAFB3* and *OsAFB5* knockout lines. Data represent the means ± SEM. Asterisks indicate significant differences (**$p < 0.01$)

contents of amylose, albumin, prolamin, and globulin and higher contents of amylopectin, total protein, and glutelin compared with Nipponbare (Fig. 6G, H and S7). These findings suggest that *OsAFB3* and *OsAFB5* may affect grain chalkiness by regulating the content of stored substances.

Subcellular localization studies of OsAFB3 and OsAFB5 were conducted in rice protoplasts. The results showed that OsAFB5 was predominantly found in the nucleus, whereas OsAFB3 was located in the cytoplasm outside the nucleus, mainly in chloroplasts (Fig. 6I, J). In rice genome, 31 Aux/IAA repressor proteins were identified (Shi et al. 2023), then, the Aux/IAA candidate interacting proteins of OsAFB3 and OsAFB5 were predicted using AlphaFold Multimer. The results showed OsIAA4, OsIAA11, OsIAA19, OsIAA26 and OsIAA8 were most likely to interact with OsAFB3; while, the most likely to interact with OsAFB5 were OsIAA4, OsIAA26, OsIAA15, OsIAA1 and OsIAA14 (Table S9). Thus, these results indicated that the molecular mechanisms underlying the involvement of OsAFB3 and OsAFB5 mediated IAA signaling pathways in rice chalkiness formation may differ.

Phenotypic Investigation of *osafb3* and *osafb5* Plants

In order to investigate the effects of *OsAFB3* and *OsAFB5* on plant growth and development, we examined the phenotypes of Nipponbare, *osafb3-5*, *osafb3-6*, *osafb5-9* and *osafb5-10* plants at maturity. The results showed that the plant height and panicle number per plant of *osafb3* and *osafb5* plants were significantly lower than Nipponbare, while, the tillering number were not significant different (Fig. 7A, B). The grain length of *osafb3* and *osafb5* were significantly longer than that in Nipponbare, however, there was no significant difference in grain width and grain thickness between Nipponbare and *OsAFB3* and *OsAFB5* knock out plants (Fig. 7C, D). The phenotype investigation results suggested that the *OsAFB3* and *OsAFB5* might play multiple roles in plant development, besides negatively regulating chalkiness in rice.

Discussion

The formation of rice endosperm involves the transportation of organic assimilates produced by functional leaves (sources) through transport tissues to grains (reservoirs). This accumulation process is constrained by three factors: the supply capacity of the source, the storage capacity of the reservoir, and the efficiency of the transport system. The coordination of this "source-flow-reservoir" relationship is crucial for preventing chalkiness. When the reservoir is large but the supply of assimilates is insufficient or/and transportation efficiency is low, chalkiness occurs (Zhou et al. 2009). In this study, the grain dimensions of HK300 were determined as follows: length, 14.83 mm; width, 3.26 mm; and thickness, 2.61 mm; but, the grain quality of HK300 was notably poor, especially in terms of chalkiness, with a chalky grain rate reaching 98.4% (Fig. 1A–M). This suggests that the reservoir of HK300 is quite large, but the source supply capacity or the transport efficiency may not adequately support the reservoir's capacity. Therefore, future strategies to improve rice quality should focus on enhancing the supply and transport capacities without altering the storage capacity, aiming to achieve high yield and high quality simultaneously.

Starch constitutes over 80% of the weight of polished rice and includes amylose and amylopectin, which are assembled into SGs (Fan et al. 2022). Thus, the proportions of amylose and amylopectin significantly affect rice quality (Zhang et al. 2016). *WCR1*, an F-box protein-encoding gene, negatively regulates rice chalkiness. Knocking out this gene results in increased grain chalkiness and reduced amylose content (Wu et al. 2022). Similarly, sucrose synthase 3 (*WBR7*), a positive regulator of chalkiness, affects rice quality; loss of *WBR7* function reduces the white-belly rate (WBR) and increases amylose content in the endosperm (Shi et al. 2024). Additionally, *OsNF-YB1* and *OsNF-YC12* interact with *OsbHLH144* to regulate *Wx* gene expression, with their knockouts leading to severe chalkiness and decreased amylose content (Bello et al. 2019). In our study, the expression levels of genes related to amylose synthesis, namely *OsGBSS1* and *OsGBSS2*, differed significantly between ZR24D and HK300 during endosperm development, with HK300 having a lower amylose content than ZR24D, whereas amylopectin content exhibited the opposite trend (Fig. 1N–P). These results suggested that the ratio of amylose to amylopectin is linked to the formation of chalkiness in HK300. Adjusting this ratio in the endosperm might enhance the quality of HK300 in future.

In plants, trehalose is primarily synthesized through the TPP/TPS pathway, which involves two steps. Initially, TPS catalyzes the glucose shift from UDPG to G6P to synthesize T6P. Subsequently, TPP dephosphorylates T6P, converting it into trehalose (Martins et al.

2013). Overexpression of rice *TPP1* gene in developing maize ears reduced the T6P concentration and increased the sucrose concentration in ear spikelets, ultimately improved the harvest index (Nuccio et al. 2015). In bread wheat, *TaTPP-6AL1* was associated with grain weight (Zhang et al. 2017). *TaTPP-7 A* enhances starch synthesis and grain filling mainly through T6P-SnRK1 pathway in wheat (Liu et al. 2023a, b). *TPP* genes has been confirmed to contribute to the difference in distribution of assimilates in sweet and grain sorghum (Li et al. 2019). So, TPP/TPS pathway has been already believed to be associated with the formation of grain-related traits. The rice genome contains 14 *TPS* and 13 *TPP* genes (Ge et al. 2008). Our results revealed differences in the expression levels and patterns of 4 *TPS* genes and 9 *TPP* genes between the two varieties during endosperm development (Fig. 4 and S6, Table S6). These findings suggested significant variations in the trehalose synthesis pathways between HK300 and ZR24D, which may contribute to the increased chalkiness in HK300 grains. Future research should explore the genes related to trehalose synthesis and the trehalose content in these varieties.

IAA is crucial for rice endosperm development, with its content sharply increasing during the early stage (1–14 DAF) of endosperm development (Xu et al. 2021). Knocking out the key genes involved in IAA biosynthesis, such as *OsTAR1*, *OsYUC9* and *OsYUC11*, led to an increase in chalkiness (Xu et al. 2021). The IAA signaling transduction pathway, well-documented in plant biology. In maize, auxin response factor, ARFTF17, regulates the expression of auxin transporter gene, *PIN1*. Null mutation of *ARFTF17* leads to an increase and dense arrangement of starch granules and protein bodies in endosperm cells (Wang et al. 2024). Although recent study has found that knocking out *OsIAA19* increases chalkiness in rice seeds, there is still limited research on the involvement of IAA signaling pathway in chalkiness formation (Jia et al. 2024). This study involved DEGs analysis, focusing on plant hormone signal transduction, to identify genes associated with ABA, BR, ET, SA, JA and IAA signaling transduction pathways. Interestingly, IAA-related DEGs outnumbered those related to the other pathways (Fig. 5, Table S8). This suggested that although the formation of chalkiness in HK300 grains is collectively regulated by multiple phytohormone interactions, the IAA signaling transduction pathway may play a predominant role in this process. Additionally, IAA receptor protein genes *OsAFB3* and *OsAFB5* knockout lines have a higher chalky grain rate highlighting the importance of IAA signaling in the formation of chalkiness (Fig. 6). Generally, grain size usually affects the chalkiness of rice and the grain length is believed in inversely proportional to the degree of chalkiness (Hu et al. 2015; Wang et al. 2015; Choi et al. 2018). In this study, we also investigated the grain size of Nipponbare, *OsAFB3* and *OsAFB5* knockout lines. The results showed that grain length of *osafb3-5*, *osafb3-6*, *osafb5-9* and *osafb5-10* plants were significantly longer than that of Nipponbare, but the grain width and grain thickness were not significantly different (Fig. 7C, D). Together, these results indicated that OsAFB3 and OsAFB5 negatively regulated chalkiness and dysfunction of *OsAFB3* and *OsAFB5* made chalkiness more severe not by regulating grain size in rice. We also utilized the multimodal protein interaction screening platform based on Alpha Fold Multimer to identify Aux/IAA proteins that may interact with OsAFB3 and OsAFB5 (Table S9). These proteins may participate in the formation of rice chalkiness. The interaction partners of OsAFB3 and OsAFB5 and the molecular mechanisms of IAA signaling pathway affecting chalkiness will be our focus of attention.

Conclusion

In this study, we systematically elucidated the possible molecular mechanisms underlying the formation of rice chalkiness, and found that the genes associated with early development of endosperm, amylose formation, and the trehalose pathway may play the major role in grain chalkiness of HK300. We also found multiple phytohormones may integrated affect the chalkiness of HK300, and confirmed that IAA receptor protein OsAFB3 and OsAFB5 negatively regulates chalkiness.

Abbreviations

IAA	Indole-3-acetic acid
TF	Transcription factor
SG	Starch granule
AGP	ADP-glucose pyrophosphorylase
GBSSI	Granule-bound starch synthase I
ADPG	Adenosine diphosphate glucose
SS	Soluble starch synthase
SBE	Starch branching enzyme
DBE	Debranching enzyme
TPS	Trehalose-6-phosphate synthase
TPP	Trehalose-6-phosphate phosphatase
ARF	Auxin response factor
pTM	Prediction template modeling
ipTM	Interface prediction template modeling
SUS	Sucrose synthase
UDP	GUDP-glucose
G1P	Glucose-1-phosphate
G6P	Glucose-6-phosphate
T6P	Trehalose-6-phosphate
BR	Brassinolide
ET	Ethylene
JA	Jasmonic acid
SA	Salicylic acid
ABA	Abscisic acid

Supplementary Information

The online version contains supplementary material available at https://doi.org/10.1186/s12284-025-00799-z.

Supplementary Material 1

Supplementary Material 2

Acknowledgements
Not applicable.

Author Contributions
Aiqing You, Lei Zhou and Guocai Yang planned the research and designed the experiments. Shaojie Shi, Huiying Wang and Wenjun Zha conducted the experiments, performed data analysis and wrote the manuscript. An Huang, Ziyi Chen, Yan Wu, Junxiao Chen, Changyan Li, Bian Wu, Sanhe Li, Huashan Xu, Peide Li, Kai Liu and Zhijun Chen provided technical assistance, drafted proposals and corrected the manuscript.

Funding
This study was supported by the Natural Science Foundation of Hubei Province (2025AFB823), National Natural Science Foundation of China (32201879), Hubei Key Laboratory of Food Crop Germplasm and Genetic Improvement (2024lzjj01), Wuhan Natural Science Foundation Exploration Program (2024040801020327), Hubei Provincial Key Research and Development Program (2023BBB031), Science and Technology Major Program of Hubei Province (2022ABA001), Wuhan Science and Technology Major Project for Biological Breeding (2022021302024850).

Data Availability
Sequence data that support the findings of this study have been deposited in the NCBI SRA database with the primary accession code PRJNA1149843.

Declarations

Ethics Approval and Consent to Participate
Not applicable.

Consent for Publication
Not applicable.

Competing Interests
The authors declare no competing interests.

Author details
[1]Laboratory of Crop Molecular Breeding, Ministry of Agriculture and Rural Affairs, Hubei Key Laboratory of Food Crop Germplasm and Genetic Improvement, Food Crops Institute, Hubei Academy of Agricultural Sciences, Wuhan 430064, China
[2]Hubei Hongshan Laboratory, Wuhan 430070, China
[3]College of Life Sciences, Wuhan University, Wuhan 430072, China

Received: 17 December 2024 / Accepted: 13 May 2025
Published online: 24 May 2025

References

Ajadi AA, Tong X, Wang H, Zhao J, Tang L, Li Z, Liu X, Shu Y, Li S, Wang S, Liu W, Tajo SM, Zhang J, Wang Y (2019) Cyclin-dependent kinase inhibitors KRP1 and KRP2 are involved in grain filling and seed germination in rice (*Oryza sativa* L). Int J Mol Sci 21(1):245
Bello BK, Hou Y, Zhao J, Jiao G, Wu Y, Li Z, Wang Y, Tong X, Wang W, Yuan W, Wei X, Zhang J (2019) NF-YB1-YC12-bHLH144 complex directly activates *Wx* to regulate grain quality in rice (*Oryza sativa* L). Plant Biotechnol J 17(7):1222–1235
Chao S, Cai Y, Feng B, Jiao G, Sheng Z, Luo J, Tang S, Wang J, Hu P, Wei X (2019) Editing of rice isoamylase gene *ISA1* provides insights into its function in starch formation. Rice Sci 26(2):77–87
Chen S, Songkumarn P, Liu J, Wang G (2009) A versatile zero background T-vector system for gene cloning and functional genomics. Plant Physiol 150(3):1111–1121
Chen C, Begcy K, Liu K, Folsom JJ, Wang Z, Zhang C, Walia H (2016) Heat stress yields a unique MADS box transcription factor in determining seed size and thermal sensitivity. Plant Physiol 171(1):606–622
Chen S, Zhou Y, Chen Y, Gu J (2018) Fastp: an ultra-fast all-in-one FASTQ preprocessor. Bioinformatics 34(17):i884–i890
Choi BS, Kim YJ, Markkandan K, Koo YJ, Song JT, Seo HS (2018) GW2 functions as an E3 ubiquitin ligase for rice expansin-like 1. Int J Mol Sci 19(7):1904
Custodio MC, Cuevas RP, Ynion J, Laborte AG, Velasco ML, Demont M (2019) Rice quality: how is it defined by consumers, industry, food scientists, and geneticists? Trends Food Sci Technol 92:122–137
Fan C, Wang G, Wang Y, Zhang R, Wang Y, Feng S, Luo K, Peng L (2019) Sucrose synthase enhances hull size and grain weight by regulating cell division and starch accumulation in Transgenic rice. Int J Mol Sci 20(20):4971
Fan P, Xu J, Wei H, Liu G, Zhang Z, Tian J, Zhang H (2022) Recent research advances in the development of chalkiness and transparency in rice. Agriculture 12:1123
Fu F, Xue H (2010) Coexpression analysis identifies rice starch regulator1, a rice AP2/EREBP family transcription factor, as a novel rice starch biosynthesis regulator. Plant Physiol 154(2):927–938
Gao J, Gao L, Chen W, Huang J, Qing D, Pan Y, Ma C, Wu H, Zhou W, Li J, Yang X, Dai G, Deng G (2024) Genetic effects of grain quality enhancement in *Indica* hybrid rice: insights for molecular design breeding. Rice (N Y) 17(1):39
Ge L, Chao D, Shi M, Zhu M, Gao J, Lin H (2008) Overexpression of the trehalose-6-phosphate phosphatase gene *OsTPP1* confers stress tolerance in rice and results in the activation of stress responsive genes. Planta 228(1):191–201
Gong J, Miao J, Zhao Y, Zhao Q, Feng Q, Zhan Q, Cheng B, Xia J, Huang X, Yang S, Han B (2017) Dissecting the genetic basis of grain shape and chalkiness traits in hybrid rice using multiple collaborative populations. Mol Plant 10(10):1353–1356
Hara T, Katoh H, Ogawa D, Kagaya Y, Sato Y, Kitano H, Nagato Y, Ishikawa R, Ono A, Kinoshita T, Takeda S, Hattori T (2015) Rice SNF2 family helicase ENL1 is essential for syncytial endosperm development. Plant J 81(1):1–12
Hirano H, Komatsu S, Nakamura A, Kikuchi F, Kajiwara H, Tsunasawa S, Sakiyama F (1991) Structural homology between semidwarfism-related proteins and glutelin seed protein in rice (*Oryza sativa* L). Theor Appl Genet 83(2):153–158
Hu J, Wang Y, Fang Y, Zeng L, Xu J, Yu H, Shi Z, Pan J, Zhang D, Kang S, Zhu L, Dong G, Guo L, Zeng D, Zhang G, Xie L, Xiong G, Li J, Qian Q (2015) A rare allele of GS2 enhances grain size and grain yield in rice. Mol Plant 8(10):1455–1465
Huang X, Peng X, Sun M (2017) OsGCD1 is essential for rice fertility and required for embryo dorsal-ventral pattern formation and endosperm development. New Phytol 215(3):1039–1058
Huang L, Tan H, Zhang C, Li Q, Liu Q (2021) Starch biosynthesis in cereal endosperms: an updated review over the last decade. Plant Commun 2(5):100237
Jia S, Ren X, Tong M, Jiang S, Zhang C, Liu Q, Li Q (2024) OsIAA19, an Aux/IAA family gene, involved in the regulation of seed-specific traits in rice. Plants (Basel) 13(24):3538
Jin S, Xu L, Leng Y, Zhang M, Yang Q, Wang S, Jia S, Song T, Wang R, Tao T, Liu Q, Cai X, Gao J (2023) The OsNAC24-OsNAP protein complex activates *OsGBSSI* and *OsSBEI* expression to fine-tune starch biosynthesis in rice endosperm. Plant Biotechnol J 21(11):2224–2240
Juan Z, Baixiao N, Zhiguo E, Chen C (2021) Towards Understanding the genetic regulations of endosperm development in rice. Chin J Rice Sci 35(4):326–341
Kabir H, Liu Q, Su Y, Huang Z, Xiao L (2017) Dynamics of phytohormones and their relationship with chalkiness of early indica rice under different post-anthesis temperature regimes. Bangladesh J Agricultural Res 42(1):2408–8293
Kolbe A, Tiessen A, Schluepmann H, Paul M, Ulrich S, Geigenberger P (2005) Trehalose 6-phosphate regulates starch synthesis via posttranslational redox activation of ADP-glucose pyrophosphorylase. Proc Natl Acad Sci U S A 102(31):11118–11123
Li Y, Wang W, Feng Y, Tu M, Wittich PE, Bate NJ, Messing J (2019) Transcriptome and metabolome reveal distinct carbon allocation patterns during internode sugar accumulation in different sorghum genotypes. Plant Biotechnol J 17(2):472–487
Li Z, Wei X, Tong X, Zhao J, Liu X, Wang H, Tang L, Shu Y, Li G, Wang Y, Ying J, Jiao G, Hu H, Hu P, Zhang J (2022) The OsNAC23-Tre6P-SnRK1a feed-forward loop regulates sugar homeostasis and grain yield in rice. Mol Plant 15(4):706–722
Liu N, Liu J, Fan S, Liu H, Zhou X, Hua W, Zheng M (2022a) An integrated omics analysis reveals the gene expression profiles of maize, castor bean, and rapeseed for seed oil biosynthesis. BMC Plant Biol 22(1):153
Liu J, Wu M, Liu C (2022b) Cereal endosperms: development and storage product accumulation. Annu Rev Plant Biol 73:255–291
Liu Z, Li P, Yu L, Hu Y, Du A, Fu X, Wu C, Luo D, Hu B, Dong H, Jiang H, Ma X, Huang W, Yang X, Tu S, Li H (2023a) OsMADS1 regulates grain quality, gene expressions, and regulatory networks of starch and storage protein metabolisms in rice. Int J Mol Sci 24(9):8017
Liu H, Si X, Wang Z, Cao L, Gao L, Zhou X, Wang W, Wang K, Jiao C, Zhuang L, Liu Y, Hou J, Li T, Hao C, Guo W, Liu J, Zhang X (2023b) *TaTPP-7A* positively feedback regulates grain filling and wheat grain yield through T6P-SnRK1 signalling pathway and sugar-ABA interaction. Plant Biotechnol J 21(6):1159–1175

Ma X, Zhang Q, Zhu Q, Liu W, Chen Y, Qiu R, Wang B, Yang Z, Li H, Lin Y, Xie Y, Shen R, Chen S, Wang Z, Chen Y, Guo J, Chen L, Zhao X, Dong Z, Liu Y (2015) A robust CRISPR/Cas9 system for convenient, high-efficiency multiplex genome editing in monocot and Dicot plants. Mol Plant 8(8):1274–1284

Martins MC, Hejazi M, Fettke J, Steup M, Feil R, Krause U, Arrivault S, Vosloh D, Figueroa CM, Ivakov A, Yadav UP, Piques M, Metzner D, Stitt M, Lunn JE (2013) Feedback Inhibition of starch degradation in Arabidopsis leaves mediated by Trehalose 6-phosphate. Plant Physiol 163(3):1142–1163

Meng Q, Zhang W, Hu X, Shi X, Chen L, Dai X, Qu H, Xia Y, Liu W, Gu M, Xu G (2020) Two ADP-glucose pyrophosphorylase subunits, OsAGPL1 and OsAGPS1, modulate phosphorus homeostasis in rice. Plant J 104(5):1269–1284

Miret JA, Griffiths CA, Paul MJ (2024) Sucrose homeostasis: mechanisms and opportunity in crop yield improvement. J Plant Physiol 294:154188

Misra G, Anacleto R, Badoni S, Butardo V, Molina L, Graner A, Demont M, Morell MK, Sreenivasulu N (2019) Dissecting the genome-wide genetic variants of milling and appearance quality traits in rice. J Exp Bot 70(19):5115–5130

Nuccio M, Wu J, Mowers R, Zhou H, Meghji M, Primavesi LF, Paul MJ, Chen X, Gao Y, Haque E, Basu SS, Lagrimini LM (2015) Expression of trehalose-6-phosphate phosphatase in maize ears improves yield in well-watered and drought conditions. Nat Biotechnol 33(8):862–869

Paul P, Dhatt BK, Miller M, Folsom JJ, Wang Z, Krassovskaya I, Liu K, Sandhu J, Yu H, Zhang C, Obata T, Staswick P, Walia H (2020) MADS78 and MADS79 are essential regulators of early seed development in rice. Plant Physiol 182(2):933–948

Ren Y, Huang Z, Jiang H, Wang Z, Wu F, Xiong Y, Yao J (2021) A heat stress responsive NAC transcription factor heterodimer plays key roles in rice grain filling. J Exp Bot 72(8):2947–2964

Shi S, Wang H, Nie L, Tan D, Zhou C, Zhang Q, Li Y, Du B, Guo J, Huang J, Wu D, Zheng X, Guan W, Shan J, Zhu L, Chen R, Xue L, Walling LL, He G (2021) *Bph30* confers resistance to brown planthopper by fortifying sclerenchyma in rice leaf sheaths. Mol Plant 14(10):1714–1732

Shi S, Zha W, Yu X, Wu Y, Li S, Xu H, Li P, Li C, Liu K, Chen J, Yang G, Chen Z, Wu B, Wan B, Liu K, Zhou L, You A (2023) Integrated transcriptomics and metabolomics analysis provide insight into the resistance response of rice against brown planthopper. Front Plant Sci 14:1213257

Shi H, Yun P, Zhu Y, Wang L, Wang Y, Li P, Zhou H, Cheng S, Liu R, Gao G, Zhang Q, Xiao J, Li Y, Xiong L, You A, He Y (2024) Natural variation of WBR7 confers rice high yield and quality by modulating sucrose supply in sink organs. Plant Biotechnol J 22(11):2985–2999

Tang W, Chen H, Zhang S, Tang J, Lin J, Fang X, Chen G, Zhang Y (2024) A novel allele in the promoter of *Wx* decreases gene expression and confers lower apparent amylose contents in *Japonica* rice (*Oryza sativa* L). Plants (Basel) 13(5):745

Wang S, Li S, Liu Q, Wu K, Zhang J, Wang S, Wang Y, Chen X, Zhang Y, Gao C, Wang F, Huang H, Fu X (2015) The OsSPL16-GW7 regulatory module determines grain shape and simultaneously improves rice yield and grain quality. Nat Genet 47(8):949–954

Wang H, Huang Y, Li Y, Cui Y, Xiang X, Zhu Y, Wang Q, Wang X, Ma G, Xiao Q, Huang X, Gao X, Wang J, Lu X, Larkins BA, Wang W, Wu Y (2024) An ARF gene mutation creates Flint kernel architecture in Dent maize. Nat Commun 15(1):2565

Wei X, Jiao G, Lin H, Sheng Z, Shao G, Xie L, Tang S, Xu Q, Hu P (2017) Grain incomplete filling 2 regulates grain filling and starch synthesis during rice caryopsis development. J Integr Plant Biol 59(2):134–153

Wu X, Liu J, Li D, Liu C (2016) Rice caryopsis development II: dynamic changes in the endosperm. J Integr Plant Biol 58(9):786–798

Wu B, Yun P, Zhou H, Xia D, Gu Y, Li P, Yao J, Zhou Z, Chen J, Liu R, Cheng S, Zhang H, Zheng Y, Lou G, Chen P, Wan S, Zhou M, Li Y, Gao G, Zhang Q, Li X, Lian X, He Y (2022) Natural variation in white-core rate 1 regulates redox homeostasis in rice endosperm to affect grain quality. Plant Cell 34(5):1912–1932

Xu X, E Z, Zhang D, Yun Q, Zhou Y, Niu B, Chen C (2021) OsYUC11-mediated auxin biosynthesis is essential for endosperm development of rice. Plant Physiol 185(3):934–950

Yan Y, Tao H, He J, Huang S (2020) The HDOCK server for integrated protein-protein Docking. Nat Protoc 15(5):1829–1852

Yang W, Liang J, Hao Q, Luan X, Tan Q, Lin S, Zhu H, Liu G, Liu Z, Bu S, Wang S, Zhang G (2021) Fine mapping of two grain chalkiness QTLs sensitive to high temperature in rice. Rice (N Y) 14(1):33

Zhang C, Zhou L, Zhu Z, Lu H, Zhou X, Qian Y, Li Q, Lu Y, Gu M, Liu Q (2016) Characterization of grain quality and starch fine structure of two *Japonica* rice (*Oryza Sativa*) cultivars with good sensory properties at different temperatures during the filling stage. J Agric Food Chem 64(20):4048–4057

Zhang P, He Z, Tian X, Gao F, Xu D, Liu J, Wen W, Fu L, Li G, Sui X, Xia X, Wang C, Cao S (2017) Cloning of *TaTPP-6AL1* associated with grain weight in bread wheat and development of functional marker. Mol Breed 37:78

Zhang H, Xu H, Feng M, Zhu Y (2018) Suppression of OsMADS7 in rice endosperm stabilizes amylose content under high temperature stress. Plant Biotechnol J 16(1):18–26

Zhang X, Tong J, Bai A, Liu C, Xiao L, Xue H (2020) Phytohormone dynamics in developing endosperm influence rice grain shape and quality. J Integr Plant Biol 62(10):1625–1637

Zhou L, Jiang L, Zhai H, Wan J (2009) Current status and strategies for improvement of rice grain chalkiness. Yi Chuan 31(6):563–572 Chinese

Publisher's Note